Electrochemical and Spectroscopic Study on the Interaction of Cytochrome *c* with Anionic Lipid Vesicles

JING, Wei-Guo(景卫国) LIU, Chang-Wei(刘长伟) TANG, Ji-Lin(唐纪琳)
WU, Zheng-Yan(吴正岩) DONG, Shao-Jun*(董绍俊) WANG, Er-Kang*(汪尔康)
State Key Laboratory of Electroanalytical Chemistry, Changchun Institute of Applied Chemistry, Chinese Academy of Sciences, Changchun, Jilin 130022, China

The structure and the electron-transfer of cytochrome *c* binding on the anionic lipid vesicles were analyzed by electrochemical and various spectroscopic methods. It was found that upon binding to anionic lipid membrane, the formal potential of cytochrome *c* shifted 30 mV negatively indicating an easier redox interaction than that in its native state. This is due to the local alteration of the coordination and the heme crevice. The structural perturbation in which a molten globule-like state is formed during binding to anionic lipid vesicles is more important. This study may help to understand the mechanism of the electron-transfer reactions of cytochrome *c* at the mitochondrial membrane.

Keywords cytochrome *c*, electrochemistry, dimyristoylphosphatidylglycerol, circular dichroism, electrospray ionization mass spectra

Introduction

Cytochrome *c* is a small cationic peripheral membrane protein which mediates single-electron transfer in the respiratory chain between cytochrome *c* reductase (Cyt red) and cytochrome *c* oxidase (Cyt ox) of the inner mitochondrial membrane. Despite extensive studies, the detailed mechanism of the electron-transfer reactions of cytochrome *c* is far from being fully understood. Most previous efforts were only directed at understanding the structure and functional properties of the form of the protein that exists at native[1-8] or denatured state.[9-13] In fact, cytochrome *c* has its special structure on mitochondrial membrane where, prior to the electron transfer, it forms complexes with Cyt ox and Cyt red and binds tightly with mitochondrial membrane. It has been well established that electrostatic interactions play a crucial role in these processes.[14]

Cytchrome *c* consists of a single polypeptide chain containing 104 amino acid residues that is covalently anchored by two thioether bonds at Cys14 and Cys17 to a hemebinding iron. The polypeptide chain is organized into a series of five α-helices and six β-turns.[15,16] The heme active site in cyt *c* consists of a 6-coordinate low-spin hemebinding His18 and Met80 in the axial ligands. The heme group, which is located in a groove and almost completely buried inside the protein, is nonplanar and is somewhat distorted into a saddle-shape geometry.[16,17] Although the exact structure of cytochrome *c* on mitochondrial membrane has not been completely understood so far, it is still an open question if the strong electrostatic forces that hold together these complexes may induce structural changes in the heme proteins and thus affect the electron-transfer pathways and mechanism.

In the present paper we analyzed the structure and the electron-transfer reactions of cytochrome *c* binding on the anionic lipid membrane by electrochemical and spectroscopic methods. The basic idea of this approach is that anionic phospholipids are the main components of mitochondrial membrane. This study can help to understand the mechanism of the electron-transfer reactions of cytochrome *c* at the mitochondrial.

Experimental

Cytochrome *c* was from horse heart (type VI, Sigma Chemical Co.), *L*-α-dimyristoylphosphatidylglycerol (DMPG) was purchased from Sigma Chemical Co. (St. Louis MO) and used without further purification. 4,4′-Dipyriyl disulfide (PySSPy) was obtained from Nakarai Ltd. Chloroform was distilled three times. All other chemicals were of analytical grade and used as obtained. All solutions were prepared with water purified by Millipore water purification set.

PySSPy (1.0 mmol·L^{-1}) was prepared in water. Aqueous solution of cytochrome *c* was prepared in 10 mmol·L^{-1} phosphate buffer at pH 7.0 with 0.1 mol·L^{-1} KCl. For the preparation of the DMPG vesicles, a dry film of 25 mg of lipid was produced under rotary evaporation from a stock solution in chloroform, which was then left under high vacuum for a minimum of 8 h to remove traces all of organic solvent. The lipid film was hydrated to desired concentration with buffer solution. The resulting multilamellar liposome suspension was sonicated until a clear suspension of small unilamellar vesicles was obtained. The vesicle sizes of a few representative samples were determined by AFM (Nanoscope III, Digital Instru-

* E-mail: ekwang@ns.ciac.jl.cn; Fax: +86-431-5689711
Received August 23, 2002; revised October 29, 2002; accepted January 20, 2003.
Project supported by the National Natural Science Foundation of China (No. 29835120).

ments, Santa Barbara, CA). The lipid vesicles had diameters ranging from 20—40 nm. Cytochrome *c* was then added into the lipid vesicles. The concentration of cytochrome *c* and the lipid/protein ratio were altered for different experiments.

Cyclic voltammetry

Cyclic voltammetry was carried out by a computer-controlled Model CS-1087 electroanalysis system (Cypress Systems, Inc., USA). The concentration of cytochrome *c* was 0.2 mmol·L^{-1} and the lipid/protein ratio was 50:1. A platinum slide was used as the counter electrode and Ag/AgCl (saturated KCl) electrode as the reference electrode. The gold electrode was constructed from gold wire (diameter 1.0 mm, 99.99%) sealed in soft glass and polished carefully with 1.0, 0.3 and 0.05 μm alumina slurry respectively. It was sonicated in water and ethanol and then cleaned with water. Prior to experiment, the electrode potential was scanned in the range of 1.5 to −0.3 V in freshly prepared deoxygenated 0.5 mol·L^{-1} H_2SO_4 solution until the voltammogram characteristic of the clean polycrystalline gold electrode was established. Freshly prepared gold electrode was put into the 1.0 mmol·L^{-1} aqueous solution of PySSPy for 24 h. All potentials were reported with respect to the reference electrode.

UV-Vis *and near*-IR *absorbance measurements*

Absorbance spectra in the Soret (350—490 nm) and the 600—750 nm regions were obtained on samples of 40 and 20 μmol·L^{-1} cytochrome *c* respectively in the presence or absence of DMPG vesicles. The lipid/protein ratio was 100:1. Spectra of the lipid-protein complexes were measured against a reference containing lipid vesicles in the same concentration as those in the same measuring cell. All spectra were recorded at room temperature on a TN6500 UV-vis spectrophotometer (Tracor Northern, USA).

Circular dichroism (CD)

CD experiments were performed with a 62 DS circular dichroism spectrometer (AVIV company, USA). Soret regions were measured using quartz cell of 1 mm optical path length. For near-UV (250—350 nm) measurements, 10 mm optical path length cells were used. Typically, a scanning rate of 50 nm/min, a time constant of 1 s, and a band width of 1.0 nm were used with 5 scans per spectrum. Spectra of lipid-protein complexes were subtracted from the background arising from the lipid vesicles alone.

Electrospray ionization mass spectra (ESI MS)

ESI MS were collected using an LCQ mass spectrometer (Finnigan Co. USA) in the positive ion mode. A Harvard Model 22 syringe pump was used to infuse the samples into the instrument at a rate of 3 μL/min. The ion spray needle was maintained at 5300 V.

Results

The gold electrode modified with PySSPy has been found to be excellent for rapid electron transfer between cytochrome *c* and the electrode.[4,6] The electrochemistry of 0.2 mmol·L^{-1} native cytochrome *c* at a sweep rate of 20 mV/s on gold electrode modified with PySSPy is shown in Fig. 1 (solid line). Cytochrome *c* exhibited a reversible redox wave by cyclic voltammetry. The formal potential ($E^{0'}$) estimated from the midpoint between anodic and cathodic peak potential is 106 mV. Both the peak separation ($\Delta E_p = 58$ mV) at the potential scan rate used and the peak current ratio obtained are close to those expected for a reversible one electron reaction. The cathodic peak current increased linearly with an increase in the square root of the potential scan rate indicating a diffusion controlled process. In Fig. 1 (dot line), it shows the cytochrome *c* electrochemistry behavior binding to the anionic lipid membrane. It is similar with native cytochrome *c*, but the $E^{0'}$ is negatively shifted to 72 mV. The decrease of the formal potential in membrane-bound state indicates the change of the structure of cytochrome *c*.

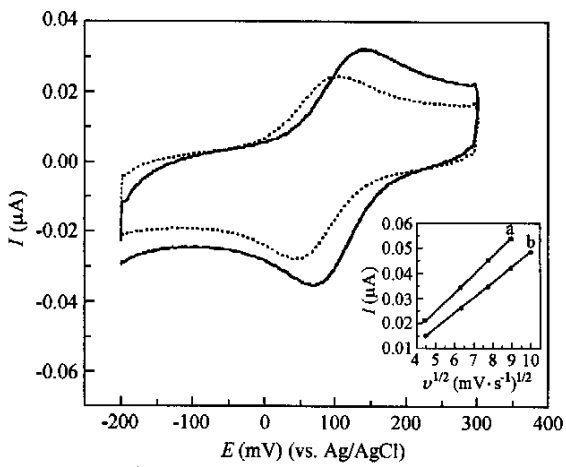

Fig. 1 Cyclic voltammograms of 0.2 mmol·L^{-1} native cytochrome *c* (solid line) and cytochrome *c* bound to DMPG vesicles (dot line) in phosphate buffer solution (pH 7.0) with 0.1 mol·L^{-1} KCl at PySSPy-modified gold electrode. Scan rate 20 mV/s. Inset: the plot of the cathodic current vs. the square root of the scan rate ($v^{1/2}$), (a) 0.2 mmol·L^{-1} native cytochrome *c*, (b) 0.2 mmol·L^{-1} cytochrome *c* bound to DMPG vesicles.

UV-Vis *and near*-IR *absorbance spectroscopy*

Cytochrome *c* is a small, heme-containing protein. The iron in the heme coordinates with two axial ligands, a histidine and a methionine. The axial coordination via the sulfur atom of methionine (Met 80) to the heme iron in cytochrome *c* results in a characteristic absorbance band at 695 nm. This S—Fe bond is not very stable. Dissociation of the Met 80 coordination can readily occur under mild denaturing condi-

tions, including pH values below 3 or above 9,[18,19] or by competitive binding of extrinsic ligands such as cyanide or imidazole.[20] On binding of cytochrome *c* to DMPG vesicles, the 695 nm band disappears (Fig. 2B). In addition, the 410 nm band characteristic of the native conformation of cytochrome *c* in aqueous solution is shifted to 407 nm (Fig. 2A).

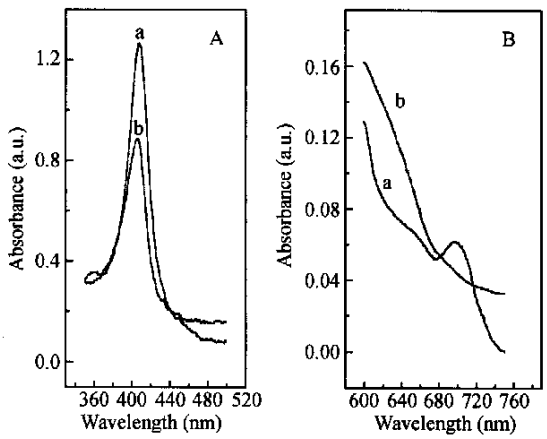

Fig. 2 Absorbance spectra of cytochrome *c* in aqueous solution (a) and when bound to DMPG vesicles (b). (A) Soret region and (B) near-IR region.

Tertiary structure change in cytochrome c upon interaction with lipid vesicles

Circular dichroism was used to monitor the effect of the interaction with lipid vesicles on the structural and conformational properties of cytochrome *c*. Fig. 3a is the far-UV CD spectrum of cytochrome *c* in 10 mmol·L^{-1} phosphate buffer at pH 7.0. The spectrum shows two pronounced minima at around 208 and 222 nm which are indicative of the high degree of α-helical in the secondary structure.[21,22] Upon binding to DMPG vesicles (Fig. 3b), no substantial change occurs in the far-UV CD band at 222 nm. It was shownpreviously that the CD signal at 222 nm is a more selective probe for the helicity because interference caused by other secondary structure elements is relatively weak at this wavelength.[23] So from the result we suggest that there is no significant change in the α-helical content. The spectral change around the minimum at 209 nm may arise from the change in other secondary structure element in the protein or may be due to the presence of optically active heme transition of the polypeptide chain.[24]

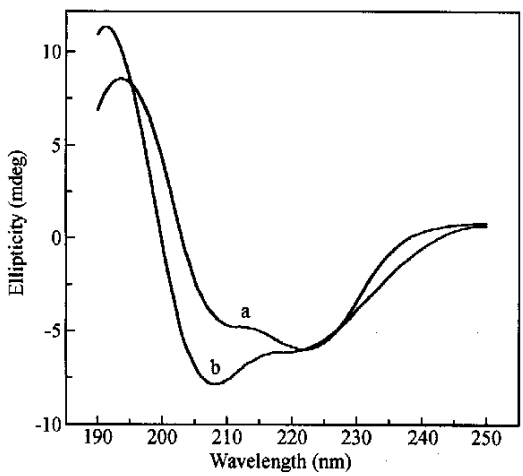

Fig. 3 Far-UV CD spectra of cytochrome *c* in phosphate buffer solution (pH 7.0) (a) and when bound to DMPG vesicles (b).

Near-UV (250—300 nm) CD is a probe for protein tertiary structure changes that affect the environment of aromatic side chain. Cytochrome *c* contains four phenylalanine residues, four tyrosine residues, one tryptophan and two thioether bonds, all of which can potentially contribute to the near-UV CD spectrum. Fig. 4a shows the near-UV spectra of cytochrome *c* in native state. It has a broad positive band at 250—270 nm and two negative bands between 280 and 290 nm. The positive band has been attributed to transitions in a heme.[25,26] The negative bands have been attributed to electronic transitions in a side chain of the single Trp 59, which has been conformed by their vanishing in a mutant where Trp 59 is replaced by Phe.[19] On binding to DMPG vesicles (Fig. 4b), these near-UV CD spectral marks of the tertiary structure disappeare which is consistent with a disruption of the tight packing of core residues in cytochrome *c* upon interaction with the lipid vesicle.[27]

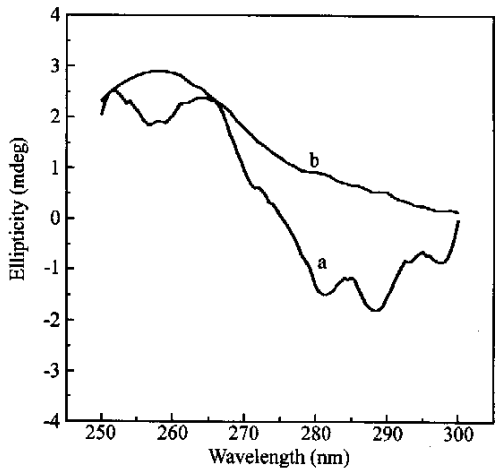

Fig. 4 Near-UV CD spectra of cytochrome *c* in phosphate buffer solution (pH 7.0) (a) and when bound to DMPG vesicles (b).

The CD spectra of cytochrome *c* in the Soret region (Fig. 5) can provide further insight into the integrity of the heme crevice.[28] The CD spectrum of cytochrome *c* in its native state (Fig. 5a) shows a strong negative limb due to the soret-cotton effect, primarily as a result of heme-polypeptide interaction.[27] After binding to the lipid membrane (Fig. 5b), the Soret CD spectrum changes to a single positive band with a maximum near 408 nm. The observed changes in the Soret region clearly indicate a disruption of the coupling between π-π^* transition of the heme group and those of the aromatic

amino acid residues in its proximity.[29] This effect is in consistent with a loosening of the tertiary structure, which removes the anisotropic character of the Soret circular dichroism band.[30]

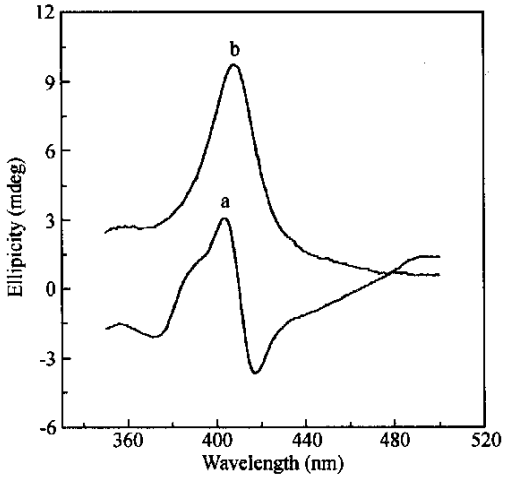

Fig. 5 CD spectrum of the Soret region of cytochrome *c* in phosphate buffer solution (pH 7.0) (a) and when bound to DMPG vesicles (b).

ESI *mass spectrum of cytochrome c in lipid vesicles*

Fig. 6 shows the ESI mass spectrum obtained from 20 $\mu mol \cdot L^{-1}$ cytochrome *c* (average MW = 12360) in 0.5 $mmol \cdot L^{-1}$ solution of ammonium acetate. In aqueous solutions of low ionic strength, cytochrome *c* is in the native state at neutral pH. The spectrum shows a single narrow distribution of peaks, with protonation states ranging from 7 + to 9 + with 8 + being the most intense and each peak corresponds to a different protonation state of cytochrome *c*. This type is typical of the ESI mass spectrum of cytochrome *c* in the native state that has been reported.[31-34] Fig. 7a shows the spectrum of pure DMPG. On binding of cytochrome *c* to DMPG vesicles, the spectrum of cytochrome *c* change remarkably (Fig. 7b). It shows a relatively wide distribution of charge states ranging from 7 + to 14 + with 10 + being the most intense, which is consistent with the ESI mass spectrum of cytochrome *c* at pH 5.2.[35] Determination of molecular mass from the mass-to-charge ratios can confirm that all the peaks designated as 7 + to 14 + arised from intact horse heart cytochrome *c*. We interpret that the changes observed in the cytochrome *c* mass spectrum result from unfolding of the protein in the anionic lipid vesicles.

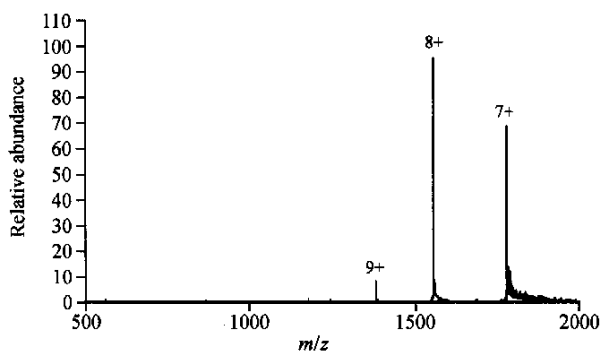

Fig. 6 Electrospray ionization mass spectrum of 20 $\mu mol \cdot L^{-1}$ horse heart cytochrome *c* in 0.5 $mmol \cdot L^{-1}$ ammonium acetate solution.

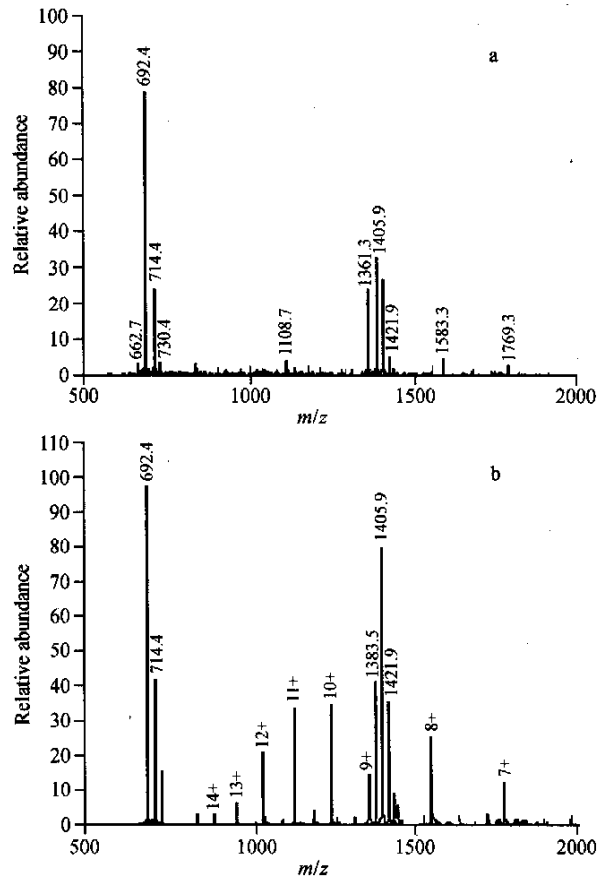

Fig. 7 Electrospray ionization mass spectra of pure DMPG (a) and DMPG containing 20 $\mu mol \cdot L^{-1}$ horse heart cytochrome *c* (b) in 0.5 $mmol \cdot L^{-1}$ ammonium acetate solution. The lipid/protein ratio was 15:1.

Discussion

Although considerable evidences exist that electrostatic interaction plays a crucial role in the redox process of cytochrome *c*, few studies of the effect of electrostatic interaction on the electron-transfer properties of cytochrome *c* have been published to date. Using surface-enhance resonance Raman spectroscopy (SERR), Hildebrandt[9] studied the structure and electron-transfer properties of cytochrome *c* adsorbed on a silver electrode/electrolyte interface, which was regarded as an appropriate model system to mimic the electrostatic interactions at the mitochondrial membrane. Recently, upon interactions with negatively charged aspartic acid peptides, Hirota[36] studied the electron-transfer reaction of cy-

tochrome *c* on PySSPy modified Au electrode. The structure of biological membrane is adaptive, liquid-crystalline supramolecular structure. The phospholipids regulate the local physicochemical properties of the membranes, such as surface charge, fluidity and curvature strain, which in turn modulate the function of membrane-associated peptides and proteins.

The formal potential of native cytochrome *c* on PySSPy modified Au electrode is 106 mV, which is in consistent with the data previously published.[7] Upon binding to DMPG, the formal potential of cytochrome *c* shifts 30 mV negatively indicating an easier electron transfer and the structural change of the protein. Upon binding to DMPG vesicles, the adsorption at 695 nm characteristic of the Met-80-iron bond disappeare, which has been interpreted as opening of the heme crevice.[17] These are in agreement with earlier results.[27] At the same time, the 410 nm band characteristic of the native conformation of cytochrome *c* in aqueous solution shifts to 407 nm indicating a transition from the low-spin state of the heme to the high-spin state.[37] This is in agreement with earlier results using static and margin angel spinning phosphorus-31 NMR which provides additional evidences for the formation of a high-spin form of cytochrome *c* in anionic lipid membranes.[38,39] Bixle[10] studied the electrochemical behavior of cytochrome *c* under different concentrations of guanidine HCl (gauHCl). The formal potential of the protein changed from 286 mV (vs. NHE) in native state to − 167 mV in unfolded state at 7 $mol \cdot L^{-1}$ gauHCl. They ascribed the low potential for the unfolded cytochrome *c* to the coordination of a single histidine to the heme. It is also observed that the same perturbation of the coordination and the open heme crevice when cytochrome *c* was bound to the anionic lipid vesicles. But the degree of the decreased formal potential is also different from that in previous reports, only from 116 mV (vs. Ag/AgCl) to 72 mV. So the alteration of the coordination and the heme crevice is not the only factor to determine the electrochemical behavior of cytochrome *c*.

Our circular dichroism results show that upon binding to the negatively charged lipid (DMPG) vesicles several features of the tertiary structure of cytochrome *c* change with no significant perturbation of the overall secondary structure (Figs. 2 and 3). Roder *et al*.[27] have used CD to investigate the interaction between cytchrome *c* and the vesicles formed by ammonic anionic phospholipid DOPS. Our CD result is consistent with what they have obtained. It suggests that both vesicles formed by DOPS and DMPG both of which are anion phospholipid and have the same interaction on cytochrome *c* studied by CD. These three features (compactness, pronounced secondary structure and strongly reduced tertiary structure) are characteristic for the molten globule state. The term of molten globule refers to a compact denatured, thermodynamically distinct state, which is believed to be an early intermediate in the pathways of protein folding both *in vivo* and *in vitro*.[40] In 1988 the molten globule state was predicated by Bychkova *et al*.,[41] and it was conformed by many experiments.[42-47] Recently studies on the interaction of cytochrome *c* with lipid membranes have suggested that a molten globule-like state was formed and a possible mechanism, a local decrease of the pH near the membrane surface, was proposed.[27] The high density of negatively charged groups on the membrane surface creates a strong electrostatic potential, which attracts protons, thus leading to a substantial decrease of the local pH at the membrane surface. However, this local decrease of pH does not exceed *ca*. 2 pH units at 0.5—1.5 nm from the membrane surface,[47] which is usually insufficient for acid denaturation and results in the molten globule-like state only. This conclusion can be further confirmed by our ESI MS results that the charge distribution of cytochrome *c* binding on anionic lipid membrane is consistent with that at pH 5.2.[35]

Cytochrome *c* is a highly polar protein. In native state, it carries + 8 or + 9 charges. Characteristically, most of the basic residues are segregated into two well-defined patches on the surface of the protein surface. But on binding to anionic lipid vesicles, cytochrome *c* carries + 10 charges (Fig. 7). This charge distribution is likely to play a crucial role in electrostatic interactions that govern the association of cytochrome *c* with liposomes and its binding to physiological redox partners on the surface of the inner mitochondrial membrane where it is easier for cytochrome *c* to transfer the electron to its redox partners.

In conclusion, upon binding to anionic lipid vesicles, cytochrome *c* undergoes a disruption of Met 80 coordination to the heme iron. The disruption of this axial coordination leads to the opening of the heme crevice. But the local changes of cytochrome *c* cannot fully account for its functional change. It is the overall destabilization of the protein structure in which a molten globule-like state is formed that results in the alteration of its electron-transfer property. The *in vivo* role of cytochrome *c* is to transfer an electron between the mitochodrial enzyme complexes, reductase and oxidase. This dynamic function requires that the protein remains in close contact and interacts with various components of the inner mitochondrial membrane. The formation of molten globule state is thus likely to be of the direct physiological relevance of cytochrome *c*.

Acknowledgments

We thank Professor Kuwana, T. (University of Kansas) for donating the CS-1087 electroanalytical system.

References

1 Eddowes, M. J.; Hill, H. A. O. *J. Chem. Soc., Chem. Commun.* **1977**, 771.
2 Eddowes, M. J.; Hill, H. A. O. *J. Am. Chem. Soc.* **1979**, *101*, 4461.
3 Myer, Y. P.; Saturno, A. F.; Verma, B. C.; Pande, A. *J. Biol. Chem.* **1979**, *254*, 11202.
4 Taniguchi, I.; Toyosawa, K.; Yamaguchi, H.; Yasukouchi, K. *J. Chem. Soc., Chem. Commun.* **1982**, 1032.
5 Willit, J. L.; Bowden, E. F. *J. Phys. Chem.* **1990**, *94*, 490.

6 Sagara, T.; Murakami, H.; Igarashi, S.; Sato, H.; Niki, K. *Langmuir* **1991**, *7*, 3190.

7 Szucs, A.; Hitchens, G. D.; Bockris, J. O. *Electrochim. Acta* **1992**, *37*, 403.

8 Cusanovich, M. A.; Meyer, T. E.; Tollin, G. *Adv. Inorg. Biochem.* **1988**, *7*, 37.

9 Hildebrandt, P.; Stockburger, M. *Biochemistry* **1989**, *28*, 6710.

10 Bixler, J.; Bakker, G.; Mclendon, G. *J. Am. Chem. Soc.* **1992**, *114*, 6938.

11 Baker, P. D.; Mauk, A. G. *J. Am. Chem. Soc.* **1992**, *114*, 3619.

12 Zhu, Y.; Dong, S. *Bioelectrochem. Bioenerg.* **1996**, *41*, 107.

13 Hamachi, I.; Fujita, A.; Kunitake, T. *J. Am. Chem. Soc.* **1997**, *119*, 9096.

14 Koppenol, W. H.; Margoliash, E. *J. Biol. Chem.* **1982**, *257*, 4426.

15 Bushnell, G. W.; Louie, G. V.; Brayer, G. D. *J. Mol. Biol.* **1990**, *214*, 585.

16 Sivakolundu, G. S.; Mabrouk, P. A. *J. Am. Chem. Soc.* **2000**, *122*, 1513.

17 Qi, P. X.; Beckman, R. A.; Wand, A. J. *Biochemistry* **1996**, *35*, 12775.

18 Dyson, H. J.; Beattie, J. K. *J. Biol. Chem.* **1982**, *257*, 2267.

19 Davies, A. M.; Guillemette, J. G.; Smith, M.; Greenwood, C.; Thurgood, A. G. P.; Mauk, A. G.; Moor, G. R. *Biochemistry* **1993**, *32*, 5431.

20 Gao, Y.; Lee, A. D. J.; Williams, R. J. P.; Williams, G. *Eur. J. Biochem.* **1989**, *182*, 57.

21 Chang, C. T.; Wu, C. S. C.; Yang, J. T. *Anal. Biochem.* **1978**, *91*, 13.

22 Myer, Y. P. *J. Biol. Chem.* **1968**, *243*, 2115.

23 Chen, Y.; Yang, J. T.; Martinez, H. M. *Biochemistry* **1972**, *22*, 4120.

24 Pinheiro, T. J. T.; Elove, G. A.; Watts, A.; Roder, H. *Biochemistry* **1997**, *36*, 13122.

25 Urry, D. W. *J. Biol. Chem.* **1967**, *242*, 4441.

26 Blauer, G.; Sreerama, N.; Woody, R. W. *Biochemistry* **1993**, *32*, 6674.

27 Pinheiro, T. J. T.; Elove, G. A.; Watts, A.; Roder, H. *Biochemistry* **1997**, *36*, 13122.

28 Myer, Y. P. *J. Biol. Chem.* 1968, *243*, 2115.

29 Santucci, R.; Giatosio, A.; Ascoli, F. *Biochim. Biophys. Acta* **1987**, *914*, 185.

30 Santucci, R.; Giatosio, A.; Ascoli, F. *Arch. Biochem. Biophys.* **1989**, *275*, 496.

31 Hamdan, M.; Curcyruto, O. *Rapid Commun. Mass Spectrom.* **1994**, *8*, 144.

32 Konermann, L.; Collings, B. A.; Douglas, D. J. *Biochemistry* **1997**, *36*, 5554.

33 Katta, V.; Chait, B. T. *J. Am. Chem. Soc.* **1991**, *113*, 8534.

34 Fenn, J. B. *J. Am. Soc. Mass Spectrom.* **1993**, *4*, 524.

35 Chowdary, S. K.; Katta, V.; Chait, B. T. *J. Am. Chem. Soc.* **1990**, *112*, 9012.

36 Hirota, S.; Masaaki, E.; Kozue, H.; Tomoya, T.; Teruhiro, T.; Takamitsu, K.; Osamu, Y. *J. Am. Chem. Soc.* **1999**, *121*, 849.

37 Konermann, L.; Douglas, D. J. *Biochemistry* **1997**, *36*, 12296.

38 Spooner, P. J. R.; Watts, A. *Biochemistry* **1991**, *30*, 3880.

39 Pinheiro, T. J. T.; Watts, A. *Biochemistry* **1993**, *33*, 2459.

40 Van der Vies, S. M.; Viitanne, P. V. *Biochemistry* **1992**, *31*, 3635.

41 Bychkova, V. E.; Pain, R. H.; Ptitsyn, O. B. *FEBS Lett.* **1988**, *238*, 231.

42 Martin, J.; Langer, T.; Boteva, R.; Schramel, A.; Horwich, A. L.; Hartl, F.-U. *Nature* **1991**, *352*, 36.

43 Van der Goot, F. G.; Lakey, J. H.; Pattus, F. *Trends Cell Biol.* **1992**, *2*, 343.

44 Van der Goot, F. G.; Gonzales-Manas, J. M.; Lakey, J. H.; Pattus, F. *Nature* **1991**, *354*, 408.

45 Bychkova, V. E.; Berni, R.; Rossi, G. L.; Kutyshenko, V. P.; Ptitsyn, O. B. *Biochemistry* **1992**, *31*, 7566.

46 Ptitsyn, O. B. *Adv. Protein Chem.* **1995**, *47*, 83.

47 Prat, M.; Teissie, J.; Tocanne, J. F. *Nature* **1986**, *322*, 756.

(E0208232 LU, Y. J.; ZHENG, G. C.)